JOURNAL OF MATERIALS SCIENCE 11 (1976) 1220–1226

G_c versus crack velocity in single groove double cantilever beam specimens of polycarbonate

R. P. KAMBOUR, S. MILLER
General Electric Company, Corporate Research and Development, Synthesis and Characterization Branch, Chemical Laboratory, Schenectady, New York, USA

The dependence of G_c on crack velocity in single-groove double cantilever beams (SG DCB) is negligible over the range of crack velocities from 0.2 to 1100 in. min^{-1}. The constancy of G_c appears to reflect a counterbalancing of the rise in yield stress by a decrease in crack opening displacement. The latter occurs through a decrease in the "gauge length" of material engulfed by yielding rather than by a decrease in the ultimate plastic strain in the crack tip plastic zone. The energy of shear lip formation at any crack velocity appears to be accurately estimated from G_c's for SG DCB specimens fractured at low velocity.

1. Introduction

In a previous paper [1] a fracture mechanics test specimen was described in which ductile crack propagation mimicked shear lip formation. The halves of plastic zone formed at the crack tip resemble shear lips closely both in geometry and degree of plastic strain. The plastic strain in BPA polycarbonate shear lips was found to be 30% as contrasted to the 60% or so for the plastic zone at the tip of a through crack in uniaxial tensile specimens and the 100% or so ultimate plastic strain characteristic of standard tensile specimens.

The test specimen is a double cantilever beam with a single side groove (SG DCB specimen) that serves to keep the crack propagation direction and the long axis of the specimen coincident. The absence of a groove on the opposite face allows shear deformation to occur in a plane normal to the direction of crack propagation. Cracks propagate smoothly with no stick-slip tendencies. As a consequence of these characteristics the crack velocity dependence of G_c under conditions that mimic shear lip formation can be assessed. This paper reports such an assessment for crack velocities from 0.2 to 1100 in. min^{-1}.

2. Experimental

All specimens were cut from as-extruded 1/8 in. thick Lexan® polycarbonate sheet ($[\eta] \simeq 0.6$ dl g^{-1}). In this study the side grooves were made with a circular slitting saw that produced a groove having a nearly rectangular profile. Groove thickness was approximately 0.025 in.

Initially a series of tests was conducted to determine the net section thickness dependence of G_c for this groove profile at a single displacement rate. Each test employed a specimen with a constant groove depth. The specimens were 2 in. wide and 6 in. long. Subsequently, a series of tests was conducted over a displacement rate range from 0.1 to 500 in. min^{-1}. In this series the groove depth of all specimens was 0.063 in. These specimens were 2 in. wide and 10 in. long for the most part.

The cracking tests at displacement rates up to 10 in. min^{-1} were conducted in an Instron Tester, the positions of the crack tip and the plastic zone tip being determined by eye with the aid of a scale marked on the specimen and recorded manually as the test proceeded. The tests at rates above 10 in. min^{-1} were carried out in an MTS closed loop hydraulic tester capable of constant displacement rates up to 6000 in. min^{-1}. Force and displacement data were stored in a Nicollet digital oscilloscope and subsequently plotted versus test time on an XY recorder. The specimen was photographed over the course of the test with a Hycam camera

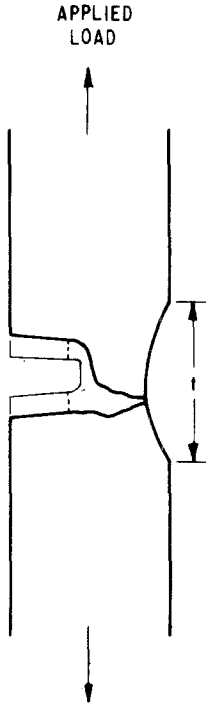

Figure 1 Section profiles of the SG DCB specimen used in the current study. Heavy line: subsequent to test. Light line: prior to test. Dotted lines: sum of these gives the plastic displacement Δt at the ungrooved surface. t = plastic zone length at surface.

capable of controlled speeds up to 6000 frames sec^{-1}. In this camera an internal mechanism marks one frame every 0.01 sec, thus allowing film speeds to be determined *a posteriori*. Selected frames from each test were projected onto a flat screen for measurement of crack lengths. From these lengths and the corresponding times crack velocities were calculated. The plastic zones were not visible in these photos due to the lighting arrangement and camera position during the test; from the low speed studies it is known, however, that the zone tip lies 0.3 in. ahead of the crack tip at the specimen surface and this was assumed to be true in the high speed tests as well.

For each test a log–log plot of δ, the displacement, divided by f, the force, versus a, the length of specimen from the loading pins to the tip of the plastic zone, was linear with a slope $n = 2.59 \pm 0.1$. The product $f\delta/a$ was found to be independent of a. Consequently, the strain energy release rate was calculated [1, 2] as

$$G_c = nf\delta/2wa$$

where w is the net section thickness through which the crack ran.

Subsequent to testing, the specimen halves were sectioned on a plane normal to the groove length and a × 10 photo taken of regions of the section surfaces adjacent to the crack. A diagram of the sectioned halves butted together is shown in Fig. 1 together with a superimposed diagram of the untested groove profile. The plastic zone thickness, t, at the ungrooved surface is determined as indicated. The corresponding plastic displacement, Δt, at the ungrooved surface is given by the difference between the original groove thickness and the length between the corresponding points on the groove faces of the broken halves (sum of the dotted lines). Plastic strains at the specimen surface were calculated as $\epsilon_p = \Delta t/t$. The plastic displacement Δg at the base of the groove is equal to Δt less the distance between the crack faces where they join the base of the groove.

3. Results

3.1. Thickness dependence of G_c and plastic zone geometry

Values of G_c taken at a displacement rate of 0.1 in. min^{-1} are plotted versus net section thickness in Fig. 2. G_c rises almost linearly with w as was the case for sharp V grooved specimens. In contrast to the latter, however, G_c extrapolates to a finite value at zero thickness. At thicknesses above 0.05 in., however, the two groove profiles give more nearly the same value of G_c.

Surface plastic zone thickness t shows the same rate of increase dt/dw as is the case in V grooved specimens. However, in the rectangular sawcut groove specimens, t extrapolates to a finite value (about 0.025 in.) at $w = 0$. Such behaviour is not surprising since the groove at its base has a similar thickness (i.e. the gauge length of the material at the root of the groove is more than 10 times as great in these specimens as in V grooved specimens). Thus, the differences in G_c at low values of w arise from the differences in groove profiles.

The dependence on thickness of the plastic displacement, at the surface Δt and at the root of the groove Δg are shown in Fig. 3. Above $w = 0.0375$ in. a given Δt is identical within experimental error to that obtained with a specimen having a 0.001 in. radius V groove of the same w (dotted line). At $w \leqslant 0.0375$ in., Δt departs from results for the V grooved specimens due to the substantial, w-independent, plastic displacement at the root of the groove. The plastic strain at the surface is thus independent of groove geometry if the net section

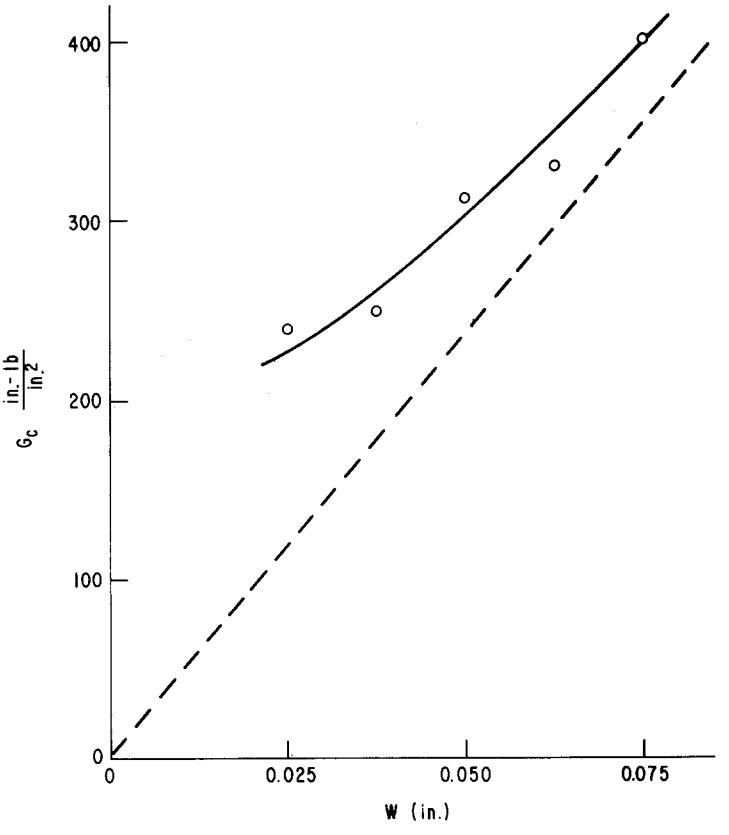

Figure 2 Dependence of G_c on net section thickness. Data: 0.025 in. sawcut grooves. Dotted line: correlation line for 0.001 in. radius V grooves [1].

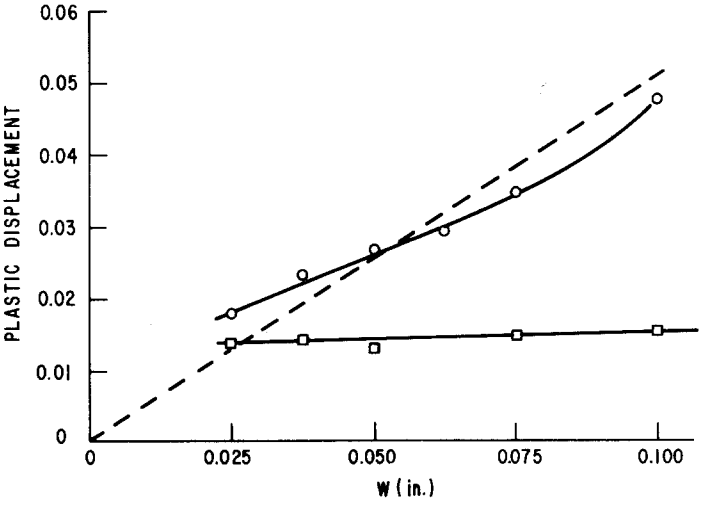

Figure 3 Plastic displacements at surface Δt and at groove base Δg versus net section thickness w. Circles: Δt. Squares: Δg. Dotted line: Δt for V grooved specimens [1].

thickness is greater than 0.0375 in. Consequently, the crack velocity dependence of G_c and ϵ_p obtained with rectangular groove specimens seems likely to be a good approximation to the crack velocity dependence of G_c and ϵ_p for V grooved specimens and thus for shear lips.

The plastic strain at the base of the groove calculated from Δg and the groove thickness at its base is 60 to 70% nominally. This estimate exceeds the true strain somewhat because Δg contains contributions from distortions outside of the 0.025 in. nominal gauge section. The evidence for this comes from cross-sections that have been cut, thinned down by standard metallographic directionless wet grinding, and polished. Fig. 4 is a transmission micrograph of such a section taken in

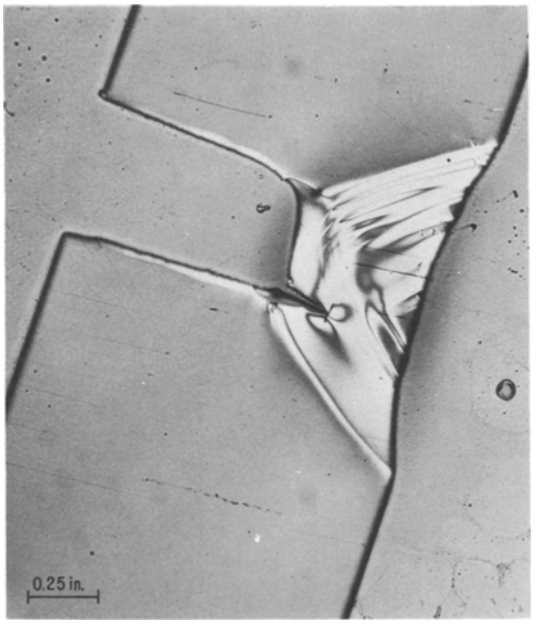

Figure 4 Transmission micrograph in partially polarized light ($\lambda = 0.54\,\mu m$) of thinned cross-section normal to specimen long axis. Section taken at such a position that plastic zone is formed but crack has advanced only part way from groove corner to surface.

partially polarized monochromatic light ($\lambda = 0.54\,\mu m$). Distortion is evident in the regions beyond the corners of the groove. It seems likely, however, that accounting for this distortion would reduce the calculated value of groove base strain to 50 or 60%. This value is higher still than the 30% characteristic of the surface due to the relatively low lateral constraints operating at the base prior to crack initiation.

3.2. Dependence of G_c and plastic zone geometry on crack velocity

With photos from each test in the series conducted over a range of displacement rates a plot was made

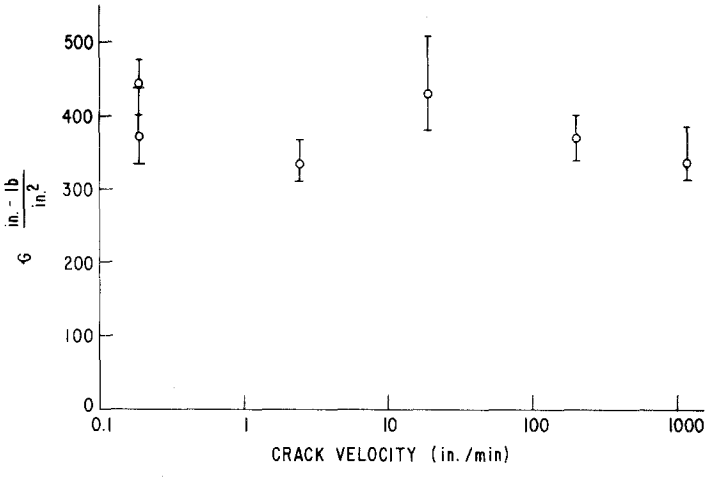

Figure 5 Average G_c versus average crack velocity. Error bars indicate ranges of values for the specimen; these reflect position dependence of each variable.

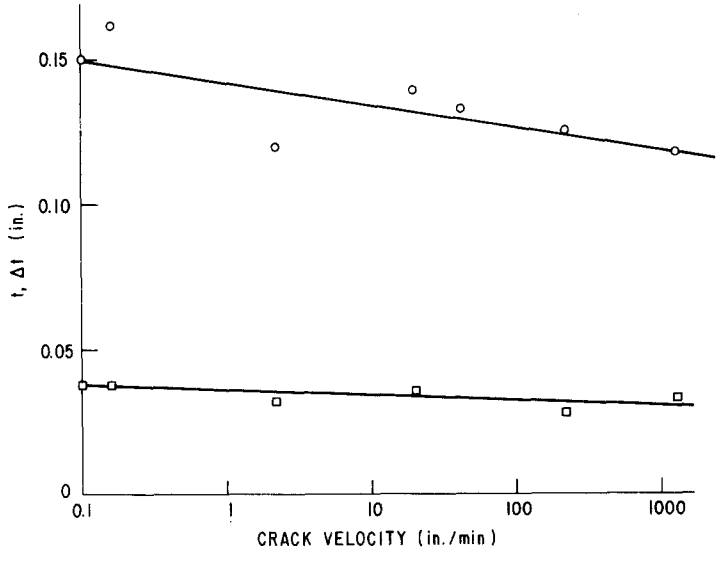

Figure 6 Thickness t and displacement Δt of plastic zone at specimen surface versus crack velocity.

of crack position versus time. A smooth curve was drawn through these data. From tangents to this curve crack velocities were calculated. Values of G_c were also plotted against time and a smooth curve drawn. Smoothed G_c values and velocity values were tabulated versus crack length. A dependence of G_c on crack length was seen; this varied in magnitude (10 to 20%) and sign from specimen to specimen. However, no dependence of G_c on crack velocity was evident within experimental error (Fig. 5).

In Fig. 6 plastic zone thickness t and plastic displacement Δt are plotted versus crack velocity. Both decrease by about 20%. Consequently, the surface strain ϵ_p is independent of velocity over the range tested.

4. Discussion

In models of ductile fracture response to stress is usually considered to be that of an ideal elastoplastic. That is, the yield stress σ_y, the drawing stress σ_d and the breaking stress σ_b are assumed to be the same and W_p the plastic work contribution to G_c is approximated as $\sigma_y \cdot \overline{\Delta t}$ where $\overline{\Delta t}$ is the average displacement in the section through which the crack runs and σ_y is the effective yield stress. Applying such a model to V grooved polycarbonate specimens [1] $\overline{\Delta t}$ was assumed to equal one half the surface displacement and σ_y was assumed equal to the plane strain yield stress. With these values the plastic work calculated was about 60% of the experimental values of G_c.

We believe, for two reasons, that better agreement (albeit partly fortuitous) between W_p and G_c could be obtained, still in the framework of the elastoplastic model. First, micrographs of the V grooved specimens analogous to Fig. 4 reveal birefringent zones having somewhat greater cross-sectional areas than those originally assumed. (As in Fig. 4 the boundary between zone and undeformed material is curved rather than linear as first assumed.) Thus, $\overline{\Delta t}$ is actually greater than $\Delta t/2$. Second, it is possible that the average effective yield stress involved in the formation of these plastic zones is greater than the plane strain yield stress; whether this is true or not depends of course on the levels of triaxial constraint operative here – a factor we cannot currently assess. Our conclusion is that $\sigma_y \overline{\Delta t}$ could have accorded better with the experimental G_c had $\overline{\Delta t}$ been more accurately assessed and had we known what the average level of triaxial constraint was. That this level of agreement would nevertheless be fortuitous will become evident below where the actual stress–strain behaviour of polycarbonate is examined.

For the moment, the lack of dependence of G_c on crack velocity (Fig. 5) can also be rationalized in terms of the elastoplastic model and the rate dependences of σ_y and $\overline{\Delta t}$. At low displacement rates the plane strain yield stress for BPA polycarbonate is 10 600 psi* [3]. The uniaxial tensile yield stress increases 600 psi/decade of strain rate [4]. If we assume that the same rate of increase is applicable under the stress configurations existing between the root of the groove and the specimen surface we calculate an increase of 23% in the yield stress over the four decades of crack velocity range in the current work. Thus, the increase in σ_y just counterbalances the decrease in $\overline{\Delta t}$ over this velocity range so that W_p is independent of crack speed.

Unfortunately, for the elastoplastic model the decrease of Δt with velocity reflects principally the change in t with velocity, the plastic strain being essentially velocity-independent. That is the yield zone engulfs less material (i.e. material further removed from the groove midplane) the greater the velocity. Insight into this behaviour can only be gained by resorting to the actual tensile stress–strain curve of polycarbonate and changes therein with temperature (Fig. 7) [5].

In the first part of drawing – that which follows the load drop at yield – drawing occurs at nearly constant stress until the shoulders of the neck reach the end of the test section of the bar. During this part the plastic strain in the neck is a constant 70% roughly. In the second part of drawing the shoulders of the neck then propagate into the grip section of the specimen, the load now rising rapidly because of the increasing cross-section of material through which the neck progresses. Note that yield stress times elongation to break gives a good approximation of total energy to failure in Fig. 7 only because of a counterbalancing of areas: the area "lost" because of the load drop following yield is compensated for by the "excess" area generated as the load rises finally toward the failure point.

Above -50° C or so more than half the total energy to break is consumed as the neck propagates into the shoulders [6]. During this process

*10^3 psi $\equiv$ 6.89 N mm^{-2}.

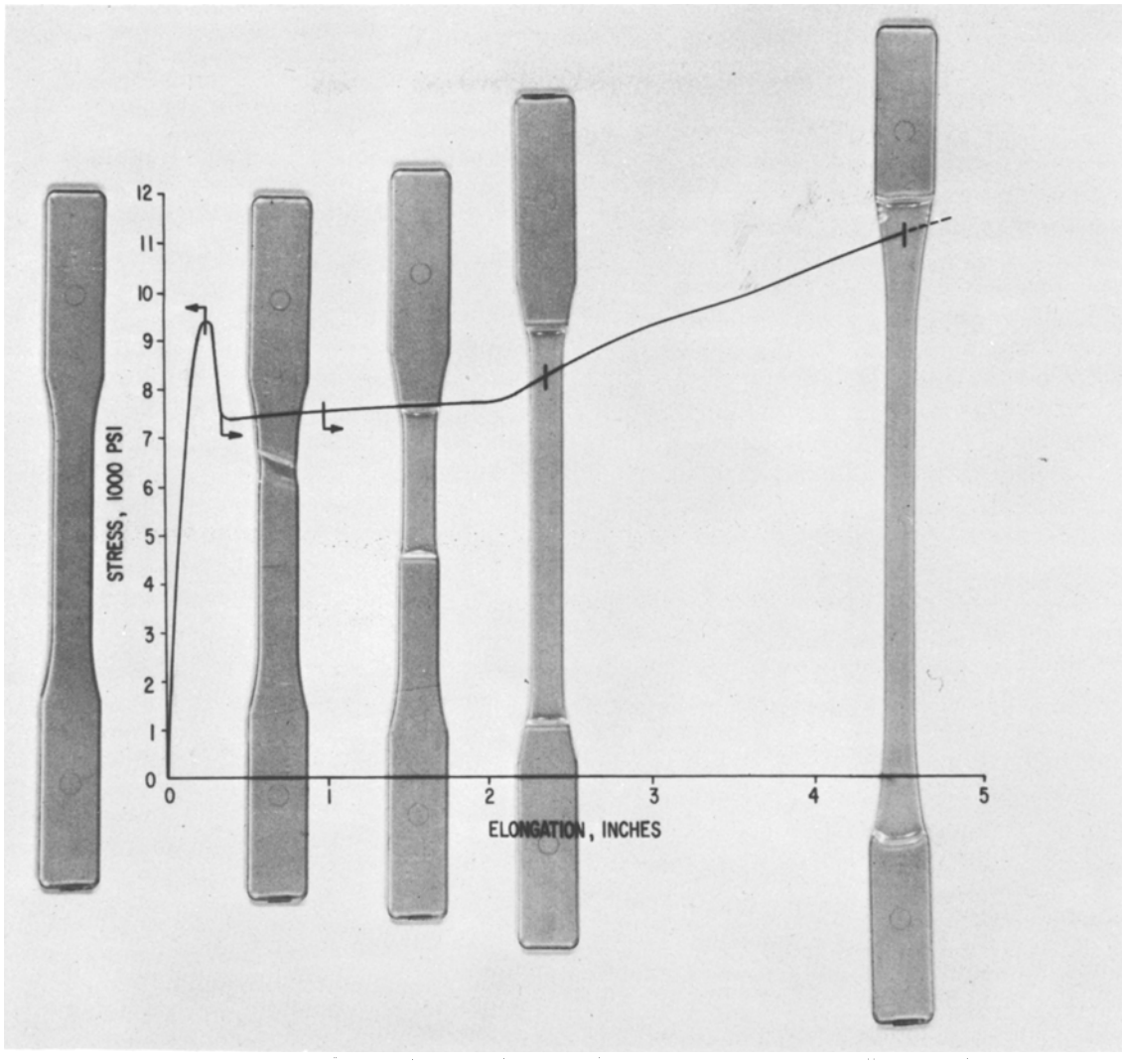

Figure 7 Engineering stress–strain curve for BPA polycarbonate, together with specimens representative of various stages of drawing [5].

the rising load results in a rising true stress and increasing plastic strain in the test section. The increase of plastic strain in the test section over the course of part two is substantial. For example, at 25° C the ultimate plastic strain in the test section increases from 70 to about 100% [7]. The fracture, when it finally occurs, is plane strain (i.e. the fracture is planar the plane meeting the surfaces of test section at right angles). As test temperature is lowered, the ultimate plastic strain in the test section and the length of grip section into which the neck has propagated both decrease [6]. Below −75° C or so propagation into the neck no longer occurs. Nevertheless, from 25 to −75° C the total work to break is constant in polycarbonate tensile tests conducted at constant displacement rate*: The increase in drawing stress with decreasing temperature is counterbalanced by the decreases of neck penetration into the grip section and attendant straining of the test section.

Thus, decreases in test temperature result in decreases of penetration of yielding into wider portions of the specimen. On the basis of the time–temperature superposition principal we expect that an increase in test speed should tend to bring a similar decrease of penetration, although uniaxial tensile data to support this conclusion do not appear to be available. Nevertheless, we

*Work to break obtained by integration of stress–strain curves (Fig. 7) of [6].

suggest that the decrease in t for the SG DCB plastic zone occurs largely for this reason.

Finally, although rather obvious, the conclusion is worth stating that the energies of forming shear lips of given sizes under high speed conditions can be closely estimated from the dependence of G_c on thickness in SG DCB specimens with sharp V grooves tested at low crack speeds.

References

1. R. P. KAMBOUR and S. MILLER, *J. Mater. Sci.* **11** (1976) 823.
2. J. P. BERRY, *J. Appl. Phys.* **34** (1963) 62.
3. R. P. KAMBOUR and R. E. ROBERTSON, in "Polymer Science", edited by A. D. Jenkins (North Holland, Amsterdam, 1972) Ch. 11.
4. A. F. YEE, W. V. OLSZEWSKI and S. MILLER, "Symposium on Toughness and Brittleness in Plastics", Am. Chem. Soc., Advances in Chemistry Series, in press.
5. C. BAUWENS-CROWET, J. C. BAUWENS and G. HOMES, *J. Mater. Sci.* 7 (1972) 176.
6. G. W. MILLER, *Polym. Prepr. Amer, Chem. Soc. Div. Polym. Chem.* 8 (1967) 1072.
7. R. A. EKVALL and J. R. LOW, JUN., *J. Appl. Polymer Sci.* 8 (1964) 1677.

Received 29 December 1975 and accepted 14 January 1976.